LIFTING-LINE THEORY FOR SUBSONIC AXIAL COMPRESSOR ROTORS

by

James E. McCune
Shashikant P. Dharwadkar

GTL Report No. 110 July 1972

GAS TURBINE LABORATORY
MASSACHUSETTS INSTITUTE OF TECHNOLOGY
CAMBRIDGE, MASSACHUSETTS

LIFTING-LINE THEORY FOR SUBSONIC AXIAL COMPRESSOR ROTORS

by

James E. McCune
Shashikant P. Dharwadkar

GTL Report No. 110 July 1972

This Research carried out in the Gas Turbine Laboratory, M.I.T., supported by NASA Lewis Research Center, under Grant No. NGL 22-009-383.

ABSTRACT

The three-dimensional compressible vortex theory of an axial compressor rotor or ducted fan is extended by relating blade loading to blade geometry in the lifting-line approximation. The resulting integral equation, which is valid up to high subsonic Mach numbers, is solved for both design and off-design problems. It is shown that three-dimensional effects must be taken into account, for rotors with non-uniform spanwise loading, in order to obtain accurate predictions of flow angles and other performance parameters.

ACKNOWLEDGEMENT

This work was supported by the NASA Lewis Research Center under Grant No. NGL 22-009-383.

The authors wish to express their appreciation to Professors J. L. Kerrebrock and J. F. Louis for many fruitful discussions. Special thanks are due Professor W. R. Hawthorne for his interest and helpful suggestions during the course of this study.

TABLE OF CONTENTS

LIST OF FIGURES

LIST OF FIGURES (cont.)

INTRODUCTION

The inviscid, three-dimensional compressible flow through an axial compressor rotor or ducted fan can be described in terms of the perturbation of the incoming flow by the rotor and its wake. If the incoming flow is sufficiently uniform and regular, and if the stator interference can be neglected as a first approximation, then the flow is steady in coordinates fixed in the rotor. If, moreover, there is negligible upstream swirl and the perturbations induced by the rotor are "small", they can be described by a velocity potential which satisfies the convected wave equation.

A useful model of the three-dimensional flow through an axial compressor blade row can be obtained by treating the duct as an infinite annulus extending upstream and downstream of the rotor. In this case, particular solutions for the potential can be found corresponding to two main types: acoustic duct modes, representing pressure and velocity fluctuations upstream and downstream of the rotor, and "far wake" solutions, analogous to those of Reissner [1], and representing wakes of shed vorticity downstream of lifting blades of variable circulation. These particular solutions can be superposed in such a way as to generate the appropriate "Green's functions" - sources, bound and shed vortices, etc. - which in turn can be used in the classical manner to develop the airfoil theory of rotor blading.

This approach to the compressible, three-dimensional aerodynamics of ducted rotors has been developed in Refs. [2]-[5]. In Refs. [2] and [3] the "thickness problem" was treated, yielding,for given blade thickness distribution, an assessment of the importance of three-dimensional effects

(as opposed to quasi-two-dimensional cascade theory), as well as a method of evaluating the wave drag of rotors in transonic operation. More recently, the lifting case has been treated [4,5], solutions for the pressure field and induced velocities being obtained for a prescribed blade loading (the "indirect" or "design" problem). It was suggested in Ref. [4] and confirmed in [5] that many features of the rotor flow field - except in the blade passages - do not depend on the details of the chordwise loading distribution but rather on its integral $\Gamma(r)$, the total blade circulation at each spanwise station. Thus, in [4], attention was focused on calculating rotor performance for specified $\Gamma(r)$, with the blades represented by B radial "spikes" of concentrated bound vorticity. Among the useful three-dimensional results of that theory is the ability to calculate the induced velocities at the blades - or lifting lines - arising both from the induction effects of the wakes of shed vorticity and from mean streamsurface shifts associated with variable work done along the blade span. However, no attempt was made in Ref. [4] to relate blade loading to blade geometry.

In the lifting surface theory of Ref. [5], for which the known bound vorticity is spread over helical surfaces representing the blades, these induced velocities were used to compute the blade camber lines associated with a specified (chordwise and spanwise) loading distribution. This is the rotor design problem, treated within the framework of linear, three-dimensional lifting surface theory. The "direct," or off-design problem, on the other hand, requires for that case the solution of a difficult multi-dimensional integral equation. An ingenious method for solution of this problem, and some preliminary results including the transonic off-design case have been given recently by Namba [6].

It is the purpose of this paper to present results for the off-design lifting problem in a framework analogous to the Prandtl lifting-line approximation of classical wing theory. As in the classical case, the idea is to modify two-dimensional theory (in this case, cascade theory) by including the induced velocities due to three-dimensional effects, insofar as they modify the local effective angle of incidence of the blading. The results obtained provide useful insight into important three-dimensional effects and their implications for rotor performance up to high subsonic relative Mach numbers. A similar (lifting-line) approach was taken by Falcao [7], for incompressible flow.

The lifting-line approximation in classical wing theory is applicable for wings of large aspect ratio. Its applicability for rotor blading in annular ducts, when typical aspect ratios (except for fans) are as low as 2 or 3, might be brought into some question. But, because of the images in the shroud and hub of the bound vorticity on the blades, the effective aspect ratio is much larger than the ratio of the actual span to chord, and the lifting-line approximation should hold quite well in subsonic flow through ducted rotors. In fact, as pointed out in a later section, we are able to check the validity of the lifting-line equation up to relative Mach numbers of 0.9 by direct comparison with the lifting-surface theory of Ref. [5].

The off-design lifting problem in the Prandtl approximation is simply stated: given the air inlet angles and blade incidence along the span, determine the spanwise distribution of blade circulation, $\Gamma(r)$. In the present development we use the two-dimensional results of Weinig [8], corrected for compressibility effects, to relate $\Gamma(r)$ to the local (effective) incidence angles - modified by the induced angles mentioned above.

The results are limited to subsonic relative Mach numbers at the rotor tips through the fact that there exists no (linear) two-dimensional theory applicable in the transonic regime. The full three-dimensional lifting surface theory [5,6] must be used in the transonic case.

The coordinate system we use in this paper is fixed in the rotor (Fig. 1); ω is the angular velocity of the rotor, U the axial velocity far upstream and r the radius. x is the axial coordinate, θ the azimuthal. The corresponding dimensionless coordinates are $(z, \theta, \sigma) \equiv (\omega x/U, \theta, \omega r/U)$.

THE PRANDTL-TYPE LIFTING LINE EQUATION

In what follows, our primary concern is to modify the actual incidence angles used in two-dimensional cascade theory to account for the induced velocities due both to streamsurface shifts and wakes of shed vorticity as predicted by the three-dimensional theory of Ref. [4]. We assume that the local lift curve slope, dC_L/di, is the same as that given by two-dimensional cascade theory; only the effective value of the incidence angle is assumed to be modified by three-dimensional effects. In the linearized approximation, in the absence of three-dimensional and compressibility effects, we would have

$$-\frac{2\Gamma(r)}{U_r c(r)} = C_L(r) = 2\pi\, K\,(\gamma,\, c/L)\cdot i \qquad (1)$$

(Fig. 2). Here, K, as obtained for incompressible flow by Weinig [8], is defined as the ratio, for the same value of i, of the lift on a blade in cascade (c/L finite) to that of the same blade in isolated flow ($c/L \to 0$). Since the lift coefficient for the latter is $2\pi i$, Eq. (1) follows in the linearized, incompressible case. Note, further, that i,

as defined by Weinig, is the incidence angle (measured from zero lift) relative to the vector mean of the upstream and downstream relative flow vectors (Fig. 2). We refer to i as the mean incidence.

Before modifying i for three-dimensional effects, we consider the effects of compressibility. For linearized, subsonic, compressible flow we can use the Prandtl-Göthert-Glauert rule, which states that the actual compressible flow (with geometry specified by γ and c/L, Fig. 2) is related to an equivalent incompressible flow such that $U_r^{inc} = U_r$ and

$$C_L(\gamma, c/L, i, \beta_r) = \frac{1}{\beta_r} C_L^{inc} [\gamma^{inc}, (c/L)^{inc}, i] \tag{2}$$

$$\tan(\gamma^{inc}) = \frac{1}{\beta_r} \tan \gamma \tag{3}$$

$$\sin \gamma^{inc} (\frac{L}{c})^{inc} = \sin \gamma (\frac{L}{c}) \tag{4}$$

where $\beta_r^2 \equiv 1 - M_r^2 = 1 - M^2/\cos^2\phi(r)$. Then Eq. (1) becomes

$$- \frac{2\Gamma(r)}{U_r c(r)} = C_L = 2\pi K(\gamma, \frac{c}{L}, \beta_r)\, i \tag{5}$$

with

$$K(\gamma, \frac{c}{L}, \beta_r) = \frac{1}{\beta_r} K^{inc}[\gamma^{inc}, (\frac{c}{L})^{inc}] \tag{6}$$

where K^{inc} is Weinig's result evaluated at γ^{inc} and $(c/L)^{inc}$ as obtained from (3) and (4). Typical values of K^{inc} are shown in Fig. 3.

As already suggested, in order to include three-dimensional effects, we consider that i in Eq. (5) must be modified to allow for the flow angles induced by downstream vorticity and streamsurface shifts. These flow angles can be obtained, as functions of $\Gamma(r)$, from the theory of

Ref. [4]. Before this can be done consistently, however, we must note some differences in the reference system used in the three-dimensional theory as opposed to that of standard two-dimensional cascade theory.

Linearized cascade theory is formulated by superposing on an "undisturbed" two-dimensional flow an infinite row of evenly spaced staggered vortices (local spacing = L) and then distributing these over the chord of each blade. The result is that the cascade, so described, produces as much upwash (or turning) upstream as downwash downstream; the disturbance field is antisymmetric about the cascade. Then the originally defined "undisturbed" reference flow direction is really the vector mean, at each spanwise station, between the (relative) flow vectors far upstream and downstream. [This is, of course, the reason that the angle i, rather than α_g (Fig. 2), appears in Weinig's theory.] Specifically, in terms of the circulation, $\Gamma(r)$, on each blade, the induced flow angles at infinity, relative to the cascade reference flow are

$$\frac{(V_{y'})^{2D}}{U_r}\ (x \to \pm\infty) = \pm\frac{\beta_r^2 \cos\phi\ \Gamma(r)}{2\beta^2\ U_r\ L(r)} \tag{7}$$

(The sign convention for Γ is such that it is negative for positive turning, Fig. 2.) In the above expressions $U_r = U/\cos\phi$ and $\beta^2 = 1 - M^2$, where M is the axial Mach number.

By contrast, in the three-dimensional vortex theory of Refs. [4] and [5], the mean upstream flow is truly undisturbed from the (relative) reference flow, $U_r = U/\cos\phi(r)$. The flow angles corresponding to (7) from the three-dimensional theory [4] are:

$$\frac{\langle V_{y'} \rangle}{U_r}(x \to -\infty) = 0$$

$$\frac{\langle V_{y'} \rangle}{U_r}(x \to +\infty) = \frac{\beta_r^2 \cos\phi}{\beta^2 U_r L}\Gamma(r) + \left(\frac{\Gamma(r) - \bar{\Gamma}}{UL\beta^2}\right)\sin^2\phi \tag{8}$$

where $\bar{\Gamma}$ is a weighted average over the span of the local circulation, proportional to the torque required to drive the rotor:

$$\bar{\Gamma} = \frac{2}{1 - h^2}\int_h^1 \eta d\eta\, \Gamma(r_T\eta) \tag{9}$$

and $\eta = r/r_T$, $h = r_H/r_T$. In Eq. (8), $\langle\rangle$ denotes an azimuthal average.

There are two main differences between the two- and three-dimensional results given by (7) and (8). The first is that, as we expect, the reference flow directions of the two theories differ by an amount

$$\alpha_{-\infty} = -\frac{\beta_r^2 \cos\phi}{2U_r L\,\beta^2}\Gamma(r) \equiv \frac{\Delta^{2D}}{2} \tag{10}$$

To obtain a common reference for the two theories, one must add this angle to any flow angle, $(V_{y'}/U_r)$, computed from the three-dimensional theory. The second difference is that the net turning of the flow in the three-dimensional theory differs from that of cascade theory by an amount proportioned to $[\Gamma(r) - \bar{\Gamma}]$. This effect has been shown [9] to be due to the mean streamsurface displacement associated with adjustments in the mean (azimuthally averaged) pressure field as the flow moves through the rotor. One-half of this incremental turning angle appears in the induced flow angle at the blades [see Eq. (14)], and this result corresponds to actuator disc theory.

We are now in a position to modify Eq. (5) to allow for three-dimensional effects. We replace i in (5) by i_{eff}, where

$$i_{eff} = i + \alpha_i \tag{11}$$

and

$$\alpha_i = \left(\frac{V_{y'}}{U_r}\right)^{ind} + \alpha_{-\infty} \tag{12}$$

Here, $(V_{y'}/U_r)^{ind}$ is the induced flow angle computed from the three-dimensional vortex theory directly, in a manner sketched briefly below, and the addition to α_i of the correction angle, $\alpha_{-\infty}$, is in accordance with the rule stated below Eq. (10).

The quantity $(V_{y'}/U_r)^{ind}$ is obtained from the theory of Ref. [4] as follows. Computing the velocity component normal to the relative wind ($V_{y'} = V_\theta \cos\phi - V_x \sin\phi$; $\tan\phi = \omega r/U$), we find its values, at each radial station, immediately upstream and downstream of a given bound vortex "spike" and take the mean of the two. (Taking the mean removes the singularity due to the bound vortex itself.) For purely subsonic flow the result is, on dividing by $U_r = U/\cos\phi\ (r)$,

$$\left(\frac{V_{y'}}{U_r}\right)^{ind} = \frac{1}{2UL(r)}\left[\Gamma(r) - \frac{\bar{\Gamma}\sin^2\phi}{\beta^2} - 2\sum_{n=1}^{\infty}\chi_n(\sigma)\right] \tag{13}$$

where $L(r) = 2\pi r/B$, $\sigma \equiv \omega r/U = \tan\phi$. Here, the $\chi_n(\sigma) \equiv \chi_{nB}(nB\sigma)$ are the "wake functions" of Ref. [4], obtained by a generalization of the method introduced by Reissner [1]. These functions represent the effect of the downstream wakes of shed vorticity and involve weighted integrals over the blade span of $d\Gamma/dr$; each $\chi_n(\sigma)$ vanishes identically when

Γ = constant = $\bar{\Gamma}$. The exact definition of the χ_n's and a means of evaluating their contribution to the induced flow angle are discussed briefly in the Appendix.

Adding $\alpha_{-\infty}$ to (13) in accordance with (12), we obtain the induced flow angle at the vortex lifting lines, in a reference frame consistent with cascade theory:

$$\alpha_i = \frac{\sin^2\phi(r)}{2UL}\left[\frac{\Gamma(r) - \bar{\Gamma}}{\beta^2} - \frac{2}{\sin^2\phi(r)}\sum_{n=1}^{\infty}\chi_n(\sigma)\right] \tag{14}$$

where we have used the identity $\beta_r^2\cos^2\phi + \sin^2\phi = \beta^2$. Finally, using (5) in its modified form, $C_L = 2\pi K i_{eff}$, we obtain the Prandtl-type lifting line equation for $\Gamma(r)$:

$$-\frac{2\Gamma(r)}{U_r c(r)} = 2\pi K\left[\, i + \frac{\sin^2\phi(r)}{2UL(r)}\left\{\left(\frac{\Gamma(r)-\bar{\Gamma}}{\beta^2}\right) - \frac{2}{\sin^2\phi}\sum_{n=1}^{\infty}\chi_n(\sigma)\right\}\,\right] \tag{15}$$

(Note that the case of a constant-work rotor reduces to the two-dimensional result, since α_i vanishes in that case. For Γ = const. there is no shed vorticity and no streamsurface shift in the linear theory.)

Before discussing this equation it is useful for our purposes to rewrite it in terms of the actual incidence angle, $\alpha_g(r)$ (Fig. 2), between the unperturbed relative flow far upstream of the blade row and the blade zero lift line at each radius. In terms of the air inlet angle, $\phi(r)$, and the blade stagger angle $\gamma(r)$, we have

$$\alpha_g = \phi(r) - \gamma(r) \tag{16}$$

On the other hand, i differs from α_g, by definition, by half the turning angle of the <u>two-dimensional</u> theory:

$$i = \alpha_g - \frac{\Delta^{2D}}{2} = \alpha_g + \frac{\beta_r^2 \cos^2\phi\Gamma(r)}{2UL\beta^2} \tag{17}$$

Then, in terms of $\alpha_g(r)$, the lifting line equation takes the form

$$-\frac{2\Gamma(r)}{U_r c(r)} = 2\pi K(\gamma,\frac{c}{L},\beta_r)\left[\alpha_g(r)+\frac{\beta_r^2\cos^2\phi\Gamma(r)}{2UL\beta^2}\right.$$

$$\left.+\frac{\sin^2\phi}{2UL}\left\{\frac{\Gamma(r)-\bar{\Gamma}}{\beta^2}-\frac{2}{\sin^2\phi}\sum_{n=1}^{\infty}\chi_n(\sigma)\right\}\right] \tag{18}$$

An equation similar to this was proposed by Falcao [7], for incompressible flow. Given the air inlet angles $\phi(r) = \tan^{-1}(\omega r/U)$ and the stagger angles, $\gamma(r)$, machined into the blading, this equation determines $\Gamma(r)$ in the lifting-line approximation. Conversely, as in the design problem, given $\phi(r)$ and $\Gamma(r)$ it becomes an (implicit) equation for the stagger angles, $\gamma(r)$, required to achieve the desired $\Gamma(r)$.

As a result of the inclusion of three-dimensional effects, Eq. (18) is an integral equation, both through the presence of the non-local quantity $\bar{\Gamma}$ and the integrals over $d\Gamma/dr$ occurring in the $\chi_n(\sigma)$ (see Appendix). In the following sections we discuss its application to the design and off-design problems of subsonic compressor theory.

SOLUTION OF THE LIFTING LINE EQUATION

Design Problem

When the axial Mach number, M, and the relative Mach number at the tips, $M_T = M/\cos\phi_T$ are specified, the air inlet angles along the blade span are fixed: $\sigma \equiv \tan\phi(r) = (r/r_T)\tan\phi_T \equiv \eta\sigma_T$, $\sigma_T = \sqrt{M_T^2 - M^2}/M$. Similarly, the local blade spacing $L(r) = \eta L_T$, and, given the blade planform, $c(r)$, and the blade spacing at the tips, L_T, the local solidity

is determined. A frequent choice for the planform is such that $c_{ax} = c \cos \gamma(r) = \text{const.}$, and this will be used in the specific examples treated below.

If, in addition to the above quantities, the blade loading, $\Gamma(r)$, is specified along the span, Eq. (18) can be used to determine the blade incidence angles required to produce the desired loading at the design condition. Note, too, that specifying $\phi(r)$ and $\Gamma(r)$ determines, through Eq. (8), the net turning of the flow through the blade row:

$$\Delta(r) = \frac{\beta_r^2 \cos^2\phi}{\beta^2 \eta} \frac{\Gamma(r)}{UL_T} + \frac{\sin^2\phi}{\beta^2\eta} \left(\frac{\Gamma(r)-\bar{\Gamma}}{UL_T}\right) \tag{19}$$

and similarly for $\Delta^{2D}(r)$, Eq. (10). Thus, on determining $\alpha_g(r)$ from (18), we also find the blade stagger angles, $\gamma(r) = \phi(r) - \alpha_g(r)$, the mean (cascade) incidence angles, $i(r) = \alpha_g - \Delta^{2D}/2$, and (given the blade camber distribution) the flow deviation angles.

Even in the design problem Eq. (18) is not an explicit equation for α_g. For example, the "lift curve slope," $2\pi K$, depends not on ϕ but on $\gamma = \phi - \alpha_g$, one of the quantities to be determined in the design; similarly, $c(r) = c_{ax}/\cos\gamma$. A simple iterative procedure can be devised, however, to overcome this difficulty. For the first iterate, one may replace γ by ϕ in $c(r)$ and $K(\gamma, \frac{c}{L}, \beta_r)$, and use (18) to calculate α_g. One then uses this result to calculate a new set of values for $\gamma(=\phi - \alpha_g)$ to be used in c and K, recalculates α_g from (18), and so on, iteratively, until convergence is obtained. In practice, convergence occurs in three to four steps.

We recognize, of course, that within the framework of a strictly linear theory no <u>a priori</u> justification of the iteration suggested above

can be given. To the same formal first-order accuracy of the theory as a whole, $K(\gamma)$ could be replaced by $K(\phi)$ and, similarly, $(c_{ax}/\cos\gamma)$ by $(c_{ax}/\cos\phi)$, since α_g is a perturbation quantity. (For that matter, ϕ could be replaced by γ in Eqs. (7) and (10) with only a second-order error.) However, we seek here an approach to the design problem which is at least intuitely consistent with the off-design cases. In the latter, we hold $\gamma(r)$ fixed and, in certain instances, vary $\phi(r)$ by varying the Mach numbers. In going from design to off-design we wish to hold $c(r) = c_{ax}/\cos\gamma$ fixed, and include in $K(\gamma,\frac{c}{L},\beta_r)$ only the variations due to changes in relative Mach number (compressibility effects). To treat K as an explicit function of ϕ in the off-design problem would be to introduce unrealistic effects. But, then, to be consistent between the design and off-design problems, we need solutions evaluated with $K = K(\gamma)$ for both cases.

The blade angles used in the above discussion are "equivalent flat plate" angles. One of the effects of blade camber appears through the choice of the zero-lift reference line. For cambered blades in cascade, a good choice for the local zero lift line is that suggested by Wislicenus [10], in which the line joining the blade trailing edge to the point of maximum camber is taken as the zero lift reference. Fig. 4 illustrates the relationship between the various equivalent flat plate angles of the present theory and those used (in a reasonably standard notation) for circular-arc blades with camber angles $\theta(r) = \kappa_1 - \kappa_2$. With the help of Wislicenus' rule, we have from Fig. 4

$$\gamma = \frac{\kappa_1 + \kappa_2}{2} .$$

Hence, specification of $\theta(r)$, together with knowledge of $\gamma(r)$, determines both κ_1 and κ_2 . The blade incidence i', normally used for cambered blades, is related to $\alpha_g(r)$ by

$$i' = \alpha_g - \frac{\theta}{2}$$

In the results presented in the following we will use for simplicity a flow deviation angle $\delta = \Delta - \alpha_g$ as defined for a flat plate cascade. However, given $\theta(r)$ and using Wislicenus' rule, we can relate this angle to the flow deviation angle commonly used for cambered blades. The result is simply

$$\delta' = \frac{\theta}{2} - \delta \cdot$$

With the help of Fig. 4, any of the equivalent flat plate angles of the present lifting-line theory can be related simply to the standard angles of a cambered blade with given $\theta(r)$, provided $\theta(r)$ is not so large as to violate a priori the assumptions of the linear theory.

In what follows, we use the design problem as a starting point, to determine a set of geometrical blade angles to be used later in the specification of the off-design problem. But the design problem can also be used here in another way. It has been treated in Ref. [5] with a lifting surface theory, which obviates several of the assumptions inherent in the lifting-line approximation. Therefore, the design problem, applied to (18), can be used to check the validity of the lifting-line equation. Such a check is illustrated in Fig. 5 for $M = 0.5$, $M_T = 0.9$, $c_{ax}/L_T = 1.06$, $B = 40$, $h = 0.8$, and a constant-work rotor. The cambered blade profiles are those computed from Ref. [5] for an assumed chordwise blade pressure loading proportional to $\sqrt{x'(c - x')}\Gamma(r)$. The equivalent flat plate angles computed from (18) for this case [$\Gamma(r) = \bar{\Gamma}$] are indicated by the straight lines. If one adopts Wislicenus' rule for

the equivalent flat plate angles of cambered blades the agreement is good; this is especially reassuring in view of the large compressibility corrections [Eqs. (2)-(4)] required at this large relative tip Mach number in obtaining the lifting-line results.

We turn now to a specific design problem, the results of which will be used to fix the blade angles used in the off-design solutions of (18) to be discussed subsequently. To illustrate, we choose $h = 0.8$, $B = 40$, $c_{ax}/L_T = 1.06$, $M = 0.5$, $M_T = 0.75$, and require that $\Gamma = \bar{\Gamma}$ (constant work) at this operating condition. For this case, Eq. (18) was solved iteratively for $\alpha_g(r)$ in the manner already described and the other angles of interest computed. Results are shown in Figs. 6, 7 and 8 for $\bar{\Gamma}/UL_T = -0.2$, corresponding to a total pressure ratio across the rotor of about 1.075. [Most of the results - α_g, Δ, δ, for example - scale (approximately) linearly with the chosen value of $\bar{\Gamma}/UL_T$.] Results for a particular type of off-design problem are also shown on these Figures; these will be discussed in the next section. It will be noted for the constant-work design case that both the required α_g and the net turning, Δ, decrease from root to tip. The latter result is due both to the free-vortex nature of the induced swirl and the increased compressibility effects [4] as the relative Mach number increases toward the tip. Because of our choice of constant work for this illustration of the design problem, the deviation angles shown in Fig. 8 for $M_T = 0.75$ are the same as those of two-dimensional (flat plate) cascade theory. As we shall see, they begin to differ substantially from two-dimensional theory as non-uniformities in $\Gamma(r)$ develop.

If in the specification of the design problem we were to choose

other than Γ = const., it would be necessary to take account of three-dimensional effects in the design. This can be done straightforwardly with the help of the last two terms on the right hand side of (18). It is important to note in this connection, however, that whatever choice is made for $\Gamma(r)$, it must be such that $d\Gamma/dr = 0$ at r_H and r_T (see Appendix) in order to obtain a finite contribution from the wake term, $\sum_n \chi_n(\sigma)$. This can lead to important differences between the required blade angles computed according to two-dimensional theory and those obtained including three-dimensional effects [Eq. (18)]. In addition, the flow angles, e.g. $\Delta(r)$ and $\delta(r)$, will show considerably more structure than the two-dimensional predictions would indicate, not unlike the structure seen in the off-design cases discussed below.

Off-Design

An important feature of the lifting-line equation lies in its applicability to the off-design case. With the blade geometry fixed - $c(r)/L(r)$ and $\gamma(r)$ specified from the design conditions - we seek to determine the variation in blade loading, $\Gamma(r)$, as well as the corresponding changes in the turning and deviation angles, as the axial and/or tip Mach numbers are changed away from the design state.

For the purposes of the present discussion, we use the design case defined above ($M = 0.5$, $M_T = 0.75$, $\Gamma = \bar{\Gamma}$) as our point of departure. The corresponding blade stagger angles, $\gamma(r)$, are given in Fig. 6, and the local solidity is determined as before: c_{ax} = const., $c_{ax}/L_T = 1.06$.

The condition that the blade stagger angles remain fixed in going from design to off-design conditions determines the new $\alpha_g(r)$ to be used in (18):

$$\gamma(r) = (\phi^D - \alpha_g^D) = [\phi^{OD}(r) - \alpha_g^{OD}(r)] \qquad (20)$$

or $\alpha_g^{OD}(r) = \phi^{OD}(r) - \gamma(r)$, where the superscripts "D" and "OD" denote design and off-design values, respectively. The new (off-design) values of $\phi^{OD}(r)$ are determined from the new values of M and M_T.

Variation in Wheel Speed at Fixed U

An off-design problem that is particularly simple conceptually is to investigate the effect of changing wheel speed at fixed axial speed (M fixed, M_T varying). While this does not correspond to moving along the normal operating line of an axial compressor, it serves to illustrate the importance of three-dimensional effects away from the design point.

Even if, as above, the design condition yields constant work ($\Gamma = \bar{\Gamma}$) we cannot expect that $\Gamma(r)$ will remain constant at any other operating condition. This being so, the three-dimensional effects included in (18)-- the terms in curly brackets-- become important. Solution of the resulting integral equation is facilitated by recognizing the role played by the various terms. The two dimensional (cascade) theory is contained in the first two terms on the right hand side of (18). The term $\sum_n \chi_n(\sigma)$ is associated with the downstream shed vorticity; interpreted as an integral operator on Γ it yields a singular kernel such that no solution of (18) is possible unless $d\Gamma/dr = 0$ at the hub and the tip (see Appendix). Physically, this is a result of the images, in the hub and shroud, of the shed vortices. This mirroring of vortices is necessary to satisfy the boundary conditions at the hub and shroud; as a result, infinite induced velocities would occur at r_H and r_T unless the strength of the shed vorticity-- proportional to $\frac{d\Gamma}{dr}$ -- vanishes there. On the other hand, for large B, the χ_n are exponentially small over the entire span

except very near the hub and tip (see Appendix), and this suggests that their effect can be neglected, as a first approximation, over nearly the whole span. The remaining term, involving $\Gamma = \bar{\Gamma}$, corresponds [9] to "actuator disc" theory (i.e., axisymmetric throughflow theory) and produces a gross effect over the whole span which is relatively easy to handle.

Since we are interested in solutions of (18) for relatively large B, an iterative procedure suggests itself. Neglecting the singular $\sum_n \chi_n(\sigma)$ term, one may solve (18) straightforwardly (as indicated below), obtaining an approximate ("actuator disc") result for $\Gamma(r)$, valid except near the hub and tip. We refer to this result as $\Gamma_{AD}(r)$. However, since this solution will not generally yield zero derivatives at r_H and r_T, it cannot be used directly to iterate in the $\sum_n \chi_n(\sigma)$ term. Instead, one must first introduce a slight modification of $\Gamma_{AD}(r)$ so as to force the required zero derivatives, and then iterate. For example, one may take

$$\Gamma^0(r) = \Gamma_{AD}(r) + \frac{(\frac{d\Gamma_{AD}}{d\sigma})_{\sigma=\sigma_H}\cosh\{B(\sigma_T-\sigma)\} - (\frac{d\Gamma_{AD}}{d\sigma})_{\sigma=\sigma_T}\cosh\{B(\sigma-\sigma_H)\}}{B\sinh\{B(\sigma_T-\sigma_H)\}}$$

which meets the requirements that $d\Gamma^0/d\sigma = 0$ at (σ_H, σ_T) and $\Gamma^0(r)$ is exponentially close to $\Gamma_{AD}(r)$ over virtually the whole center span. When $\Gamma^0(r)$ is used to iterate in the $\sum_n \chi_n(\sigma)$ item, convergence to a complete solution of (18) is quite rapid provided $B \gtrsim 10$. The result confirms that the main effect of the wake terms is to flatten out $\Gamma(r)$ near r_H and r_T.

To illustrate the method of solution of (18) without the wake term, we note that when $\sum_n \chi_n(\sigma)$ is neglected we can solve for $\Gamma(r) = \Gamma_{AD}(r)$ in terms of $\alpha_g(r)$ and $\bar{\Gamma}$ to obtain

$$\Gamma_{AD}(r) = A(r)\alpha_g(r) + B(r)\,\bar{\Gamma}_{AD} \tag{21}$$

where A(r) and B(r) involve K, c_{ax}/L_T, $\phi(r)$ and $\gamma(r)$. Then

$$\bar{\Gamma}_{AD} = \overline{A(r)\alpha_g(r)} + \overline{B(r)}\,\bar{\Gamma}_{AD}$$

where $\overline{(\quad)} = [2/(1-h^2)]\int_h^1 \eta d\eta\,(\quad)$, $\eta \equiv r/r_T$. Thus,

$$\bar{\Gamma}_{AD} = \frac{\overline{A\alpha_g}}{1-\bar{B}} \tag{22}$$

and, from (21),

$$\Gamma_{AD}(r) = A(r)\alpha_g(r) + \frac{B(r)}{1-\bar{B}}\,\overline{A\alpha_g} \tag{23}$$

This solution, corresponding to an "actuator disc" approximation, is shown in Fig. 6 for the off-design Mach numbers M_T = 0.7, 0.8 and 0.9. For comparison, we also show the results corresponding to two-dimensional cascade theory (Γ_{2D}), obtained from (18) by neglecting all three-dimensional effects.

As M_T is increased at fixed M, the blade incidence increases and the magnitude of Γ/UL_T increases markedly from the design value (taken in this example as -0.2). At the same time, a definite slope, $d\Gamma/dr$, develops, leading to significant three-dimensional effects. In particular, it will be noted that, at M_T = 0.9, the three-dimensional effects,

which are themselves due to a non-uniformity in Γ, act in such a way as to reduce that non-uniformity. Thus, they provide a sort of relieving effect as one departs from design conditions.

The full three-dimensional results, including wake effects calculated by the iterative method outlined above, are also shown in Fig. 6. As expected, they differ from $\Gamma_{AD}(r)$ primarily in their vanishing derivatives at r_H and r_T. It will be noted that the wake terms have very little effect on $\overline{\Gamma}$ and hence [4] on the pressure ratio of the rotor. On the other hand, as shown in Figs. 7 and 8, the wake effects have significant implications for the flow turning angles. In the "actuator disc" results, at $M_T = 0.9$, $|\Gamma_{AD} - \overline{\Gamma}|$ increases from hub to tip sufficiently rapidly to completely reverse the trend of the turning angles (hub to tip) from that predicted by two-dimensional theory. A similar result was noted in Ref. [5]. The wake terms provide a significant relieving of this effect near the hub and tip, but in the center of the span the full three-dimensional results are still well approximated by those derived from $\Gamma_{AD}(r)$.

The relieving effect of the wake terms, relative to "actuator disc" flow angles, can also be seen in Fig. 8. At $M_T = 0.9$ there is, for example, much less overturning of the flow at the tips than would be predicted from "actuator disc" theory alone. This effect can be understood by realizing that between each pair of discrete wakes of shed vorticity there is a cell of circulating potential flow which strongly modifies the mean flow angle distribution. This can be thought of as a sort of "secondary flow."

Change in Wheel Speed at Constant Air Inlet Angle

In normal operation of an axial compressor an increase in wheel speed is accompanied by an increase in the axial throughflow in such a way that the air inlet angles-- and consequently, the blade incidence angles-- remain approximately constant. We use this condition to define a second off-design problem which is perhaps more realistic than the one just discussed. Starting from the same design point ($M_T = 0.75$, $M = 0.5$), we consider the effect of varying M_T at fixed ϕ_T.

In this case the solutions of (18) would remain unchanged from those of the design ($\Gamma = \bar{\Gamma}$) but for the effects of compressibility which enter through β and β_r. The method of solution in the off-design case is exactly the same as that just discussed, and we turn directly to a discussion of the solutions.

Results for $\Gamma(r)$ as obtained from (18) in the various approximations indicated are shown in Fig. 9. On comparison of the two dimensional and full three dimensional results for $M_T = 0.6$ and 0.9 we see once again that the effects of both the streamsurface shifts and induced velocities due to the wakes is to reduce the non-uniformities which cause them. Indeed, in this case the actual fractional deviation across the span, $(\Gamma_{3D}(r_T) - \Gamma_{3D}(r_H)/\bar{\Gamma}_{3D}$, is only about 15% at $M_T = 0.9$ as compared with just over 40% according to two-dimensional theory. At the same time, $\bar{\Gamma}_{2D} \cong \bar{\Gamma}_{3D}$.

These results have an interesting implication for the turning angles [see Eq. (19)] for this particular off-design case. Since $(\Gamma - \bar{\Gamma})$ remains small in the three-dimensional result, and $\bar{\Gamma}_{2D} \cong \bar{\Gamma}_{3D}$, the turning angles

predicted by the two theories will be approximately the same. This is confirmed in Fig. 10. In contrast to the results shown in Fig. 7, the trend, hub-to-tip, for the turning angles in Fig. 10 is similar in two-dimensional and three-dimensional theory.

There are some noticeable differences, however, in the details of the turning angle distribution, as one must expect from the large difference between $\Gamma_{2D}(r)$ and $\Gamma_{3D}(r)$ at $M_T = 0.9$ (Fig. 9). These are displayed more clearly in the deviation angles, $\delta(r) = \Delta(r) - \alpha_g(r)$, plotted in Fig. 11. We notice, at $M_T = 0.9$, that the "actuator disc" results predict increased underturning over the inner semi-span and considerable overturning at the outer radii. Once again, the effect of the wake terms is to relieve these effects, both at the tips and at the hub.

SUMMARY AND CONCLUSIONS

The three-dimensional compressible vortex theory of an axial compressor rotor [4] has been extended by relating the blade loading to blade geometry in a lifting-line approximation valid up to high subsonic Mach numbers. The resulting Prandtl-type lifting-line equation can be used either to determine blade angles required to produce a given loading (the design problem), or to calculate the rotor loading and performance parameters for a given geometry over a variety of operating conditions (the off-design problem). Within the limitations of linear inviscid theory, the lifting-line method offers a unified, self-consistent procedure for including in design and performance calculations not only the effects predicted by cascade and by axisymmetric throughflow

theories but also those predictable only from a full three-dimensional approach to the problem.

Specifically, we have found that the lifting-line theory describes two important non-local effects not included in two-dimensional cascade theory. The first such effect corresponds to "actuator disc" theory and involves mean streamsurface shifts which affect both the mean flow angles and the effective incidence of the blades by changing the mean value of the axial component of velocity. The second effect is associated with the discrete wakes of vorticity shed from blades of variable circulation. These wakes set up cells of circulating potential flow between them which also significantly modify both the effective blade incidence and the flow turning angles.

Both of these effects operate so as to reduce any non-uniformities in the spanwise distribution of circulation which may develop as operating conditions change. The streamsurface deflections, at the higher tip Mach numbers, produce a tendency toward overturning over the outer half span and underturning in the inner region. The discrete wake effect, on the other hand, strongly counteracts this tendency, reducing the turning in the immediate vicinity of the tips and increasing it at the hub. For rotors operating with variable work it appears to be important to include the wake effect in order to obtain an accurate prediction of the flow angles.

APPENDIX

The complete expression for each wake function, $\chi_n(\sigma)$, is given in Ref. [4] as

$$\chi_n(\sigma) \equiv \chi_{nB}(nB\sigma) = \frac{K'(\sigma_T)I'(\sigma_H)K(\sigma) - K'(\sigma_T)K'(\sigma_H)I(\sigma)}{K'(\sigma_T)I'(\sigma_H) - K'(\sigma_H)I'(\sigma_T)} \int_{\sigma_H}^{\sigma_T} \hat{\sigma} d\hat{\sigma} I'(\hat{\sigma}) \frac{d\Gamma}{d\hat{\sigma}}$$

$$+ \frac{I'(\sigma_T)K'(\sigma_H)I(\sigma) - I'(\sigma_H)I'(\sigma_T)K(\sigma)}{K'(\sigma_T)I'(\sigma_H) - K'(\sigma_H)I'(\sigma_T)} \int_{\sigma_H}^{\sigma_T} \hat{\sigma} d\hat{\sigma} K'(\hat{\sigma}) \frac{d\Gamma}{d\hat{\sigma}}$$

$$+ I(\sigma) \int_{\sigma_H}^{\sigma} \hat{\sigma} d\hat{\sigma}\ K'(\hat{\sigma}) \frac{d\Gamma}{d\hat{\sigma}} - K(\sigma) \int_{\sigma_H}^{\sigma} \hat{\sigma} d\hat{\sigma}\ I'(\hat{\sigma}) \frac{d\Gamma}{d\hat{\sigma}} \qquad (24)$$

where $I(\sigma) \equiv I_{nB}(nB\sigma)$, $K(\sigma) \equiv K_{nB}(nB\sigma)$ are the modified Bessel functions of the first and second kind, and we have used the notation

$$I'(\sigma) \equiv (d/d\sigma) I_{nB}(nB\sigma) \ , \ K'(\sigma) \equiv (d/d\sigma)\ K_{nB}(nB\sigma) \ .$$

Each $\chi_n(\sigma)$ depends on the blade number B through its appearance both in the order and the argument of the Bessel functions.

For $B \gtrsim 10$ advantage can be taken of the approximate expressions for the modified Bessel functions of large order due to Nicholson [11]. Using Nicholson's formulas, introducing the variable $\tau \equiv \sqrt{1 + \sigma^2}$, and neglecting terms of order $(nB\tau^3)^{-1}$ compared to unity, we find we can carry out the complete sum $\sum_{n=1}^{\infty} \chi_n(\sigma)$ occurring in (18) to obtain

$$\sum_{n=1}^{\infty} \chi_{nB}(nB\sigma) \cong -\frac{1}{2}\int_{\sigma_H}^{\sigma_T} d\hat{\sigma}\left(\frac{\hat{\tau}}{\tau}\right)^{1/2} \frac{d\Gamma}{d\hat{\sigma}} \frac{\left(\frac{\tau_T+1}{\tau_T-1}\right)^{B}\left(\frac{\tau-1}{\tau+1}\right)^{B/2}\left(\frac{\hat{\tau}-1}{\hat{\tau}+1}\right)^{B/2} e^{-2B\left(\tau_T-\frac{\tau+\hat{\tau}}{2}\right)}}{1-\left(\frac{\tau_T+1}{\tau_T-1}\right)^{B}\left(\frac{\tau-1}{\tau+1}\right)^{B/2}\left(\frac{\hat{\tau}-1}{\hat{\tau}+1}\right)^{B/2} e^{-2B\left(\tau_T-\frac{\tau+\hat{\tau}}{2}\right)}}$$

$$+\frac{1}{2}\int_{\sigma_H}^{\sigma_T} d\hat{\sigma}\left(\frac{\hat{\tau}}{\tau}\right)^{1/2} \frac{d\Gamma}{d\hat{\sigma}} \frac{\left(\frac{\tau_H-1}{\tau_H+1}\right)^{B}\left(\frac{\tau+1}{\tau-1}\right)^{B/2}\left(\frac{\hat{\tau}+1}{\hat{\tau}-1}\right)^{B/2} e^{-2B\left(\frac{\tau+\hat{\tau}}{2}-\tau_H\right)}}{1-\left(\frac{\tau_H-1}{\tau_H+1}\right)^{B}\left(\frac{\tau+1}{\tau-1}\right)^{B/2}\left(\frac{\hat{\tau}+1}{\hat{\tau}-1}\right)^{B/2} e^{-2B\left(\frac{\tau+\hat{\tau}}{2}-\tau_H\right)}}$$

$$+\frac{1}{2}\int_{\sigma}^{\sigma_T} d\hat{\sigma}\left(\frac{\hat{\tau}}{\tau}\right)^{1/2} \frac{d\Gamma}{d\hat{\sigma}} \frac{\left(\frac{\tau-1}{\tau+1}\right)^{B/2}\left(\frac{\hat{\tau}+1}{\hat{\tau}-1}\right)^{B/2} e^{B(\tau-\hat{\tau})}}{1-\left(\frac{\tau-1}{\tau+1}\right)^{B/2}\left(\frac{\hat{\tau}+1}{\hat{\tau}-1}\right)^{B/2} e^{B(\tau-\hat{\tau})}}$$

$$-\frac{1}{2}\int_{\sigma_H}^{\sigma} d\hat{\sigma}\left(\frac{\hat{\tau}}{\tau}\right)^{1/2} \frac{d\Gamma}{d\hat{\sigma}} \frac{\left(\frac{\tau+1}{\tau-1}\right)^{B/2}\left(\frac{\hat{\tau}-1}{\hat{\tau}+1}\right)^{B/2} e^{-B(\tau-\hat{\tau})}}{1-\left(\frac{\tau+1}{\tau-1}\right)^{B/2}\left(\frac{\hat{\tau}-1}{\hat{\tau}+1}\right)^{B/2} e^{-B(\tau-\hat{\tau})}} \qquad (25)$$

The singularities at $\hat{\tau} = \tau$ in the two incomplete integrals, when added together, form a Cauchy principal value analogous to that occurring in classical lifting line theory and thus present no problems when due care is taken in the computational work. On the other hand, if $\tau = \tau_T$ ($\sigma = \sigma_T$), the first complete integral is genuinely singular and a finite value for $\sum_n \chi_n(\sigma)$ is possible only if $d\Gamma/d\sigma$ vanishes as $\sigma \to \sigma_T$. Similarly, the second complete integral is singular if $\tau = \tau_H$, and this requires $(d\Gamma/d\sigma)_{\sigma=\sigma_H} = 0$ for a finite contribution from the wake terms. These requirements are reflected in the solutions discussed in the text.

REFERENCES

1. Reissner, H., "On the Vortex Theory of the Screw Propellor," J. Aeronautical Sciences, 5, 1, Nov. 1937.

2. McCune, J. E., "A Three-Dimensional Theory of Axial Compressor Blade Rows -- Application in Subsonic and Supersonic Flows", J. Aero/Space Sci. 25, 544, 1958.

3. McCune, J. E., "The Transonic Flow Field of an Axial Compressor Blade Row", J. Aero/Space Sci. 25, 616, 1958.

4. Okurounmu, O., and McCune, J. E., "Three-Dimensional Vortex Theory of Axial Compressor Blade Rows at Subsonic and Transonic Speeds," AIAA J., 8, 7, July 1970.

5. Okurounmu, O., and McCune, J. E., "Transonic Lifting Surface Theory for Axial Flow Compressors," United Aircraft Corp. Res. Labs Rep. UAC K213580-1, March 1971.

6. Namba, M., "Small Disturbance Theory of Rotating Subsonic and Transonic Cascades," 1st Int. Symp. on Air Breathing Engines, Marseille, France, June 1972.

7. Falcao, A. F. de O., "Three-Dimensional Flow Analysis in Axial Turbomachines," Ph.D. Thesis, Eng. Dept., Cambridge University, Aug. 1970.

8. Weinig, F. S., "Theory of Two-Dimensional Flow Through Cascades," in Aerodynamics of Turbines and Compressors, W. R. Hawthorne, ed., Princeton Series on High Speed Aerodynamics and Jet Propulsion, X, Princeton Univ. Press, 1964.

9. McCune, J. E., and Okurounmu, O., "Three-Dimensional Flow in Transonic Axial Compressor Blade Rows," Int. Symp. on Fluid Mechanics and Design of Turbomachinery, Pennsylvania State Univ., Sept. 1970. Proceedings to appear in NASA SP 304, B. Lakshminarayana, ed., U. S. Government Printing Office, Washington, D.C., 1972.

10. Wislicenus, G., Fluid Mechanics of Turbomachines, 1, Dover Publications, New York, 1965.

11. Nicholson, J. W., "The Approximate Calculation of Bessel Functions of Imaginary Arguments," Philosophical Magazine, Ser. 6, 20.

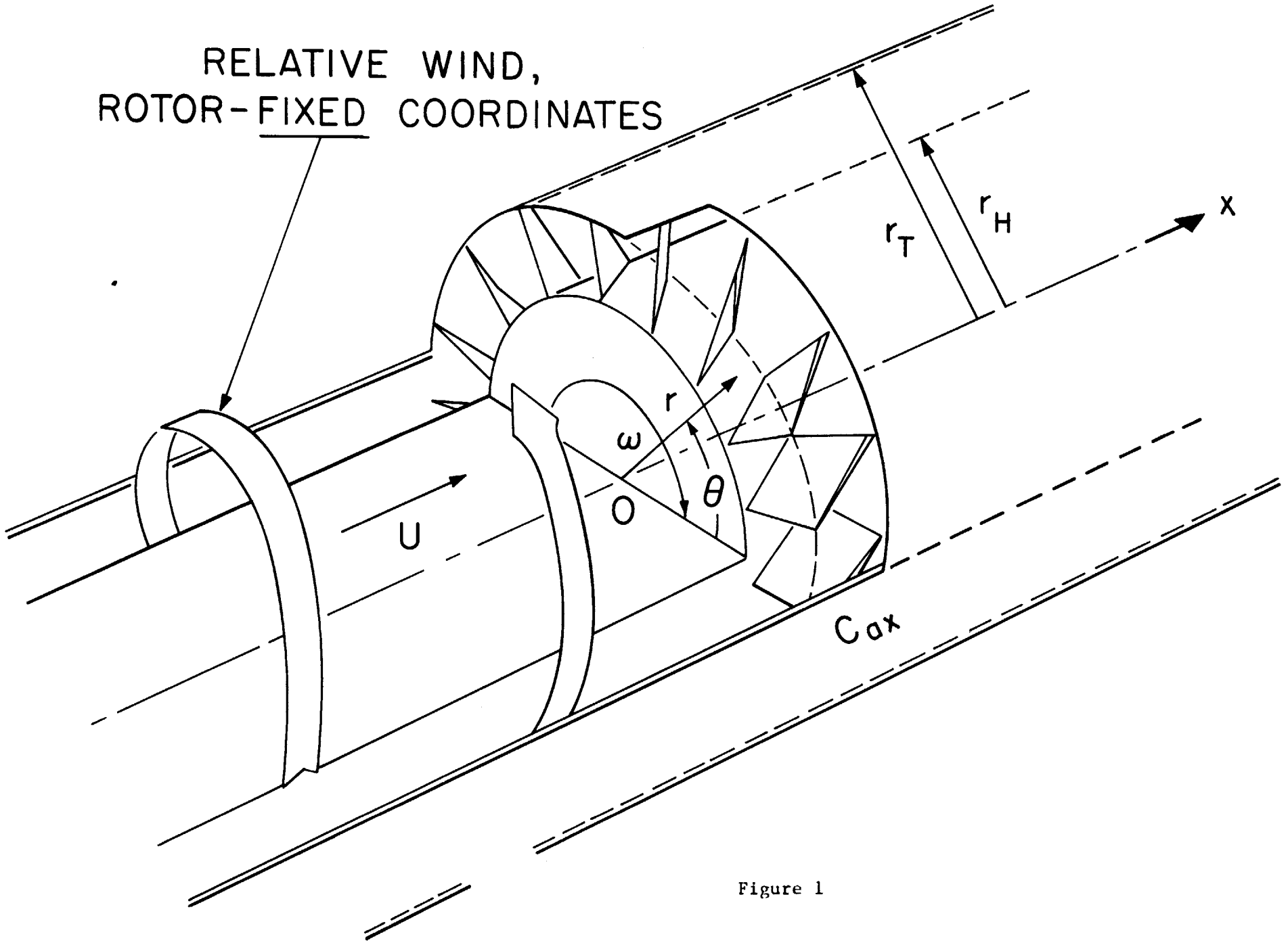

Figure 1

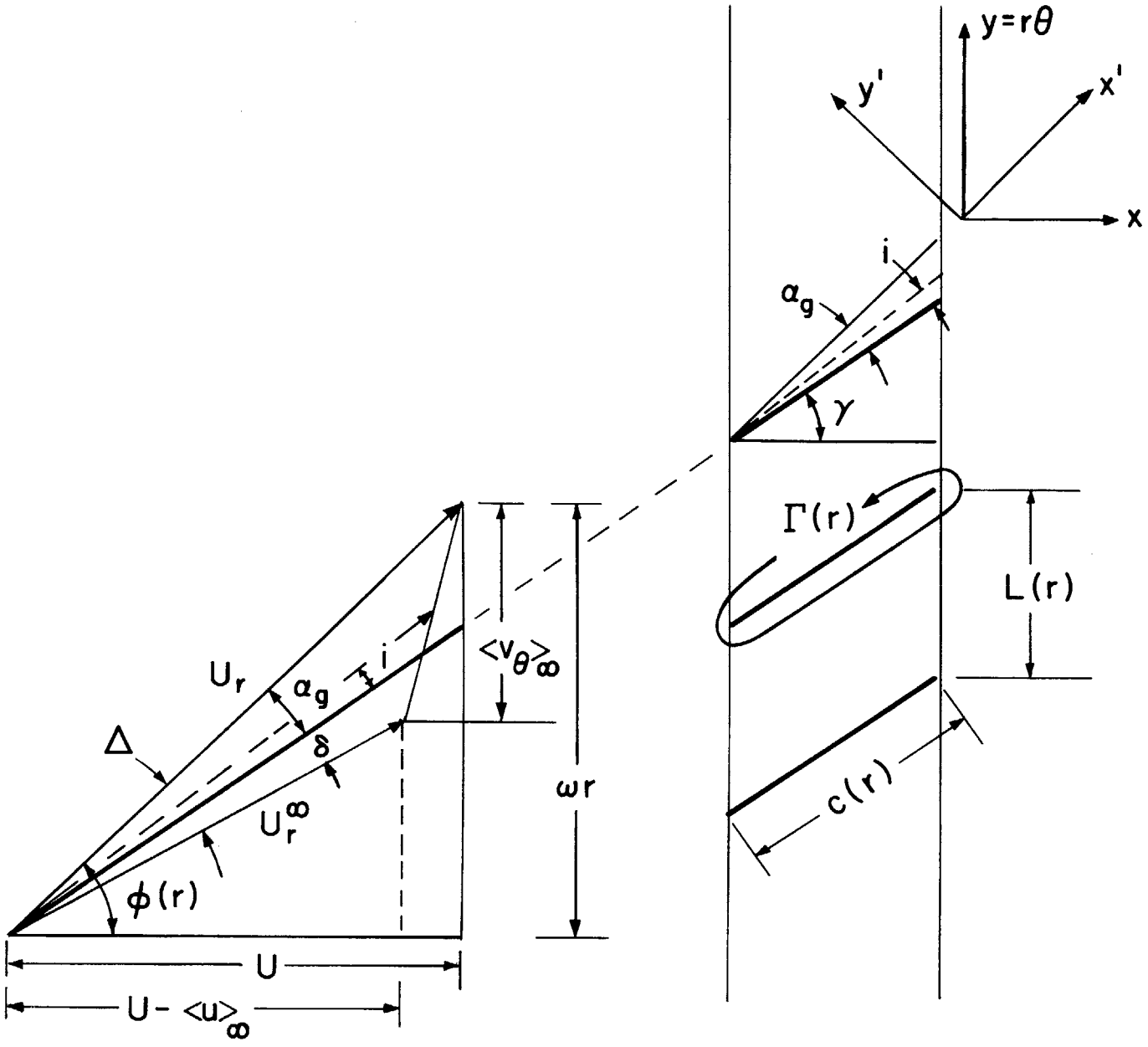

$$\tan \phi = \sigma = \frac{\omega r}{U}$$

Figure 2

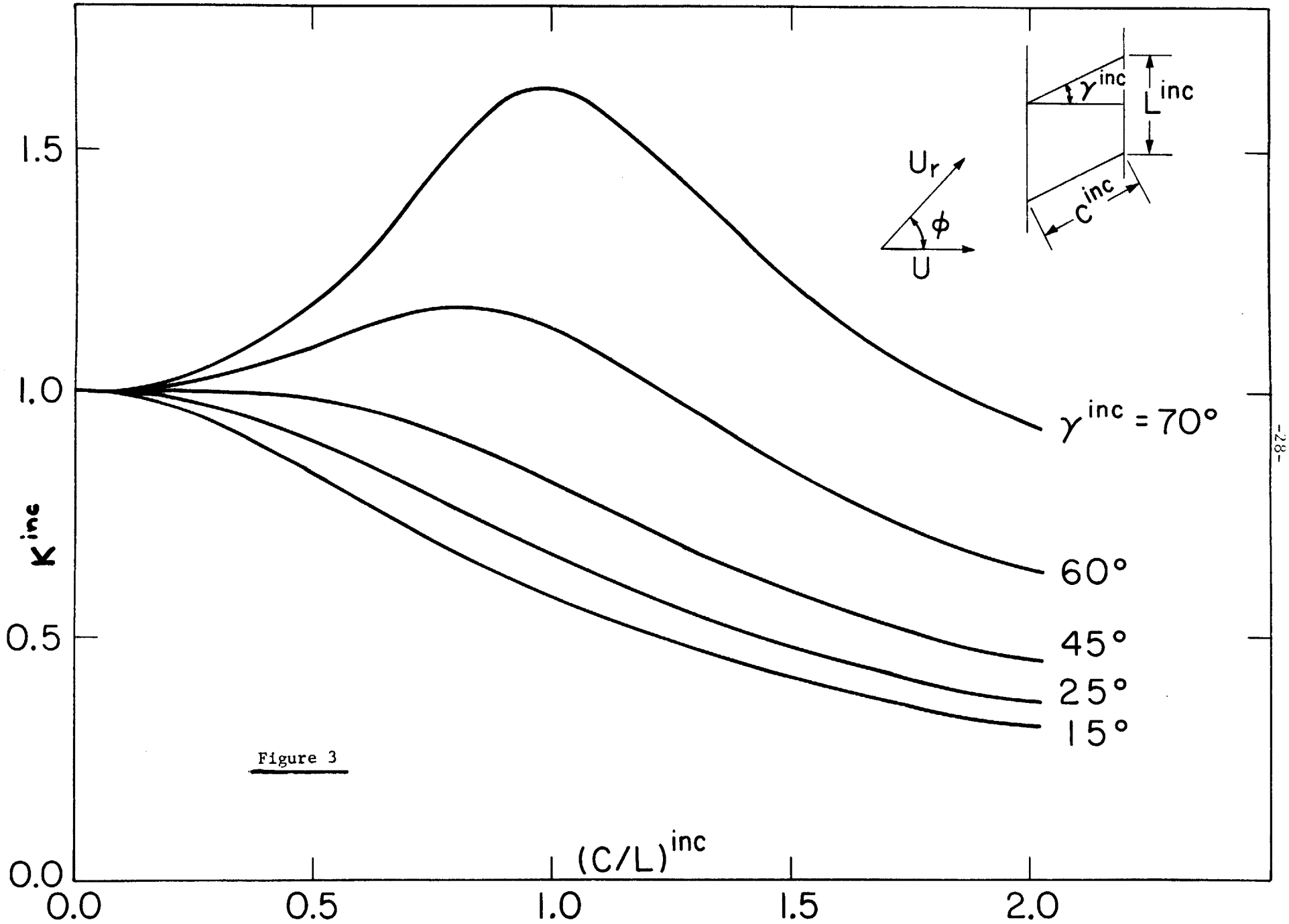
1.5
1.0
0.5
0.0
K^{inc}
0.0
0.5
1.0
1.5
2.0
$(C/L)^{inc}$
$\gamma^{inc} = 70°$
60°
45°
25°
15°
U_r
ϕ
U
γ^{inc}
L
inc
C^{inc}

Figure 3

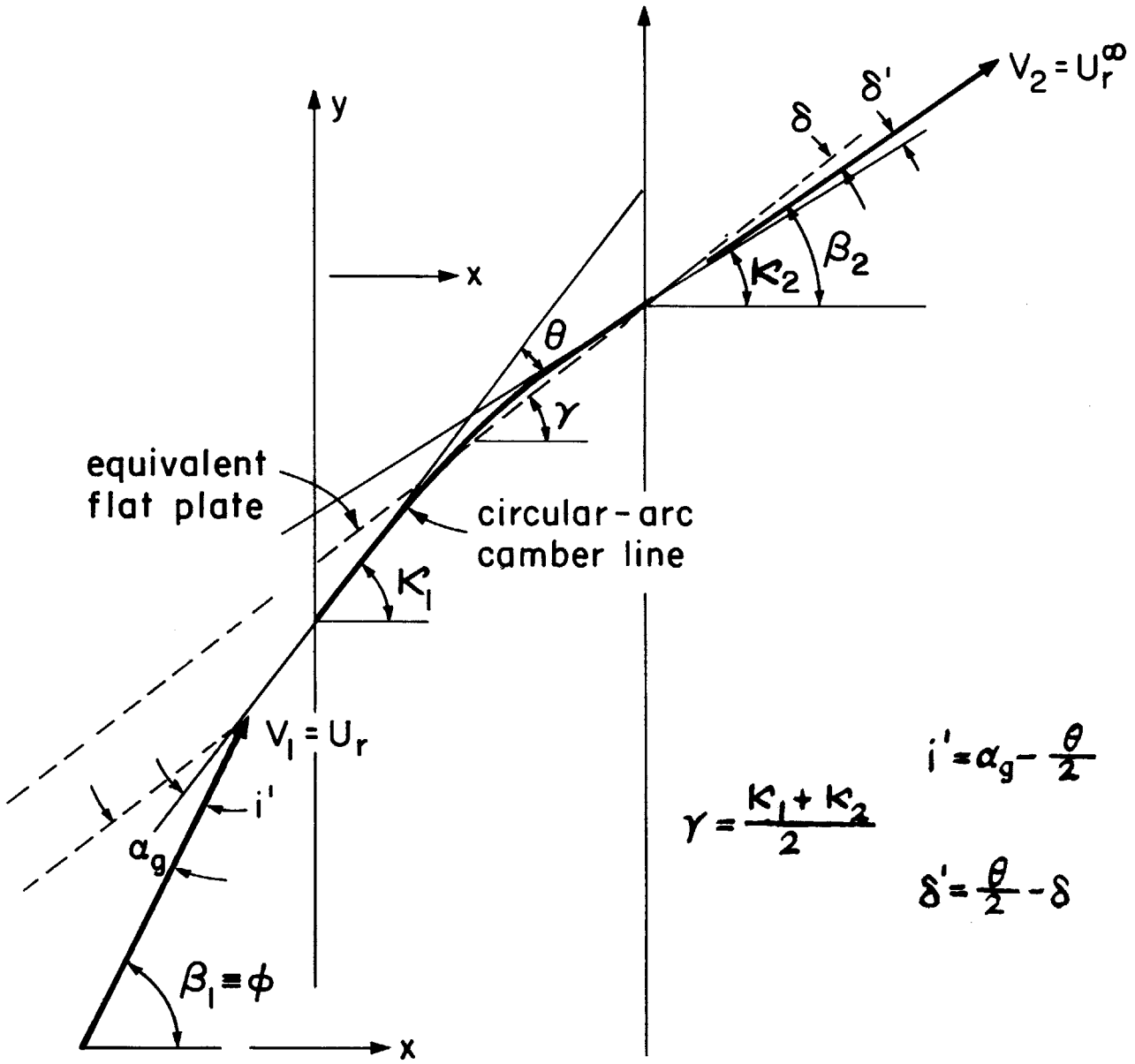
y
x
$V_2 = U_r^\infty$
δ'
δ
β_2
κ_2
θ
γ
equivalent
flat plate
circular-arc
camber line
κ_1
$V_1 = U_r$
i'
α_g
$\beta_1 \equiv \phi$
x
δ'
$i' = \alpha_g - \frac{\theta}{2}$
$\gamma = \frac{\kappa_1 + \kappa_2}{2}$
$\delta' = \frac{\theta}{2} - \delta$

Figure 4

$B = 40,\ h = .8,\ C_{ax} / L_T = 1.06,\ M = .5,\ M_T = 0.9$

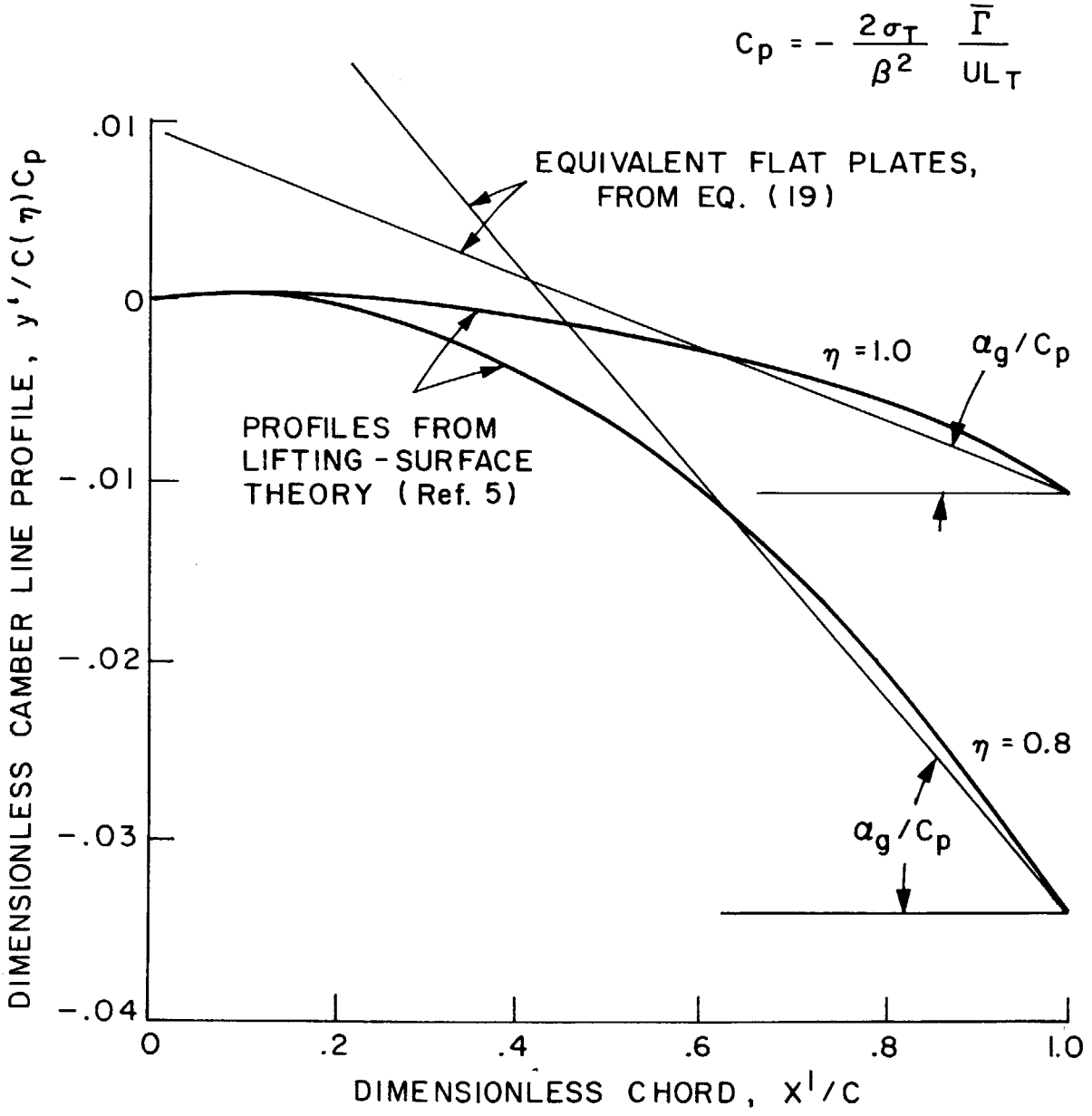

Figure 5

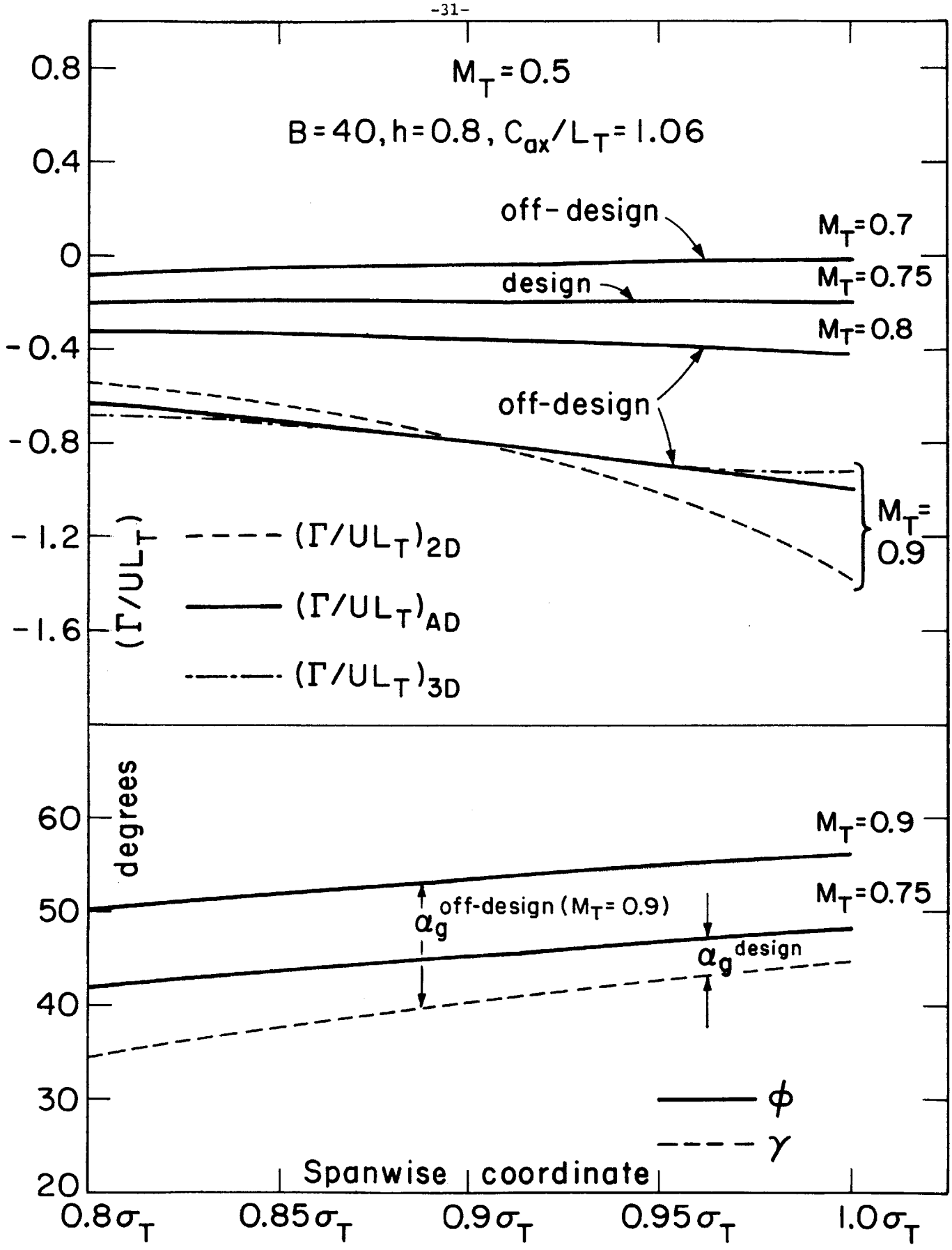
$M_T = 0.5$
$B = 40, h = 0.8, C_{ax}/L_T = 1.06$
off-design
design
$M_T = 0.7$
$M_T = 0.75$
$M_T = 0.8$
off-design
$M_T = 0.9$
$(\Gamma/UL_T)_{2D}$
$(\Gamma/UL_T)_{AD}$
$(\Gamma/UL_T)_{3D}$
(Γ/UL_T)
0.8
0.4
0
-0.4
-0.8
-1.2
-1.6
degrees
60
50
40
30
20
$M_T = 0.9$
$M_T = 0.75$
α_g off-design ($M_T = 0.9$)
α_g design
ϕ
γ
Spanwise coordinate
$0.8\sigma_T$
$0.85\sigma_T$
$0.9\sigma_T$
$0.95\sigma_T$
$1.0\sigma_T$

Figure 6

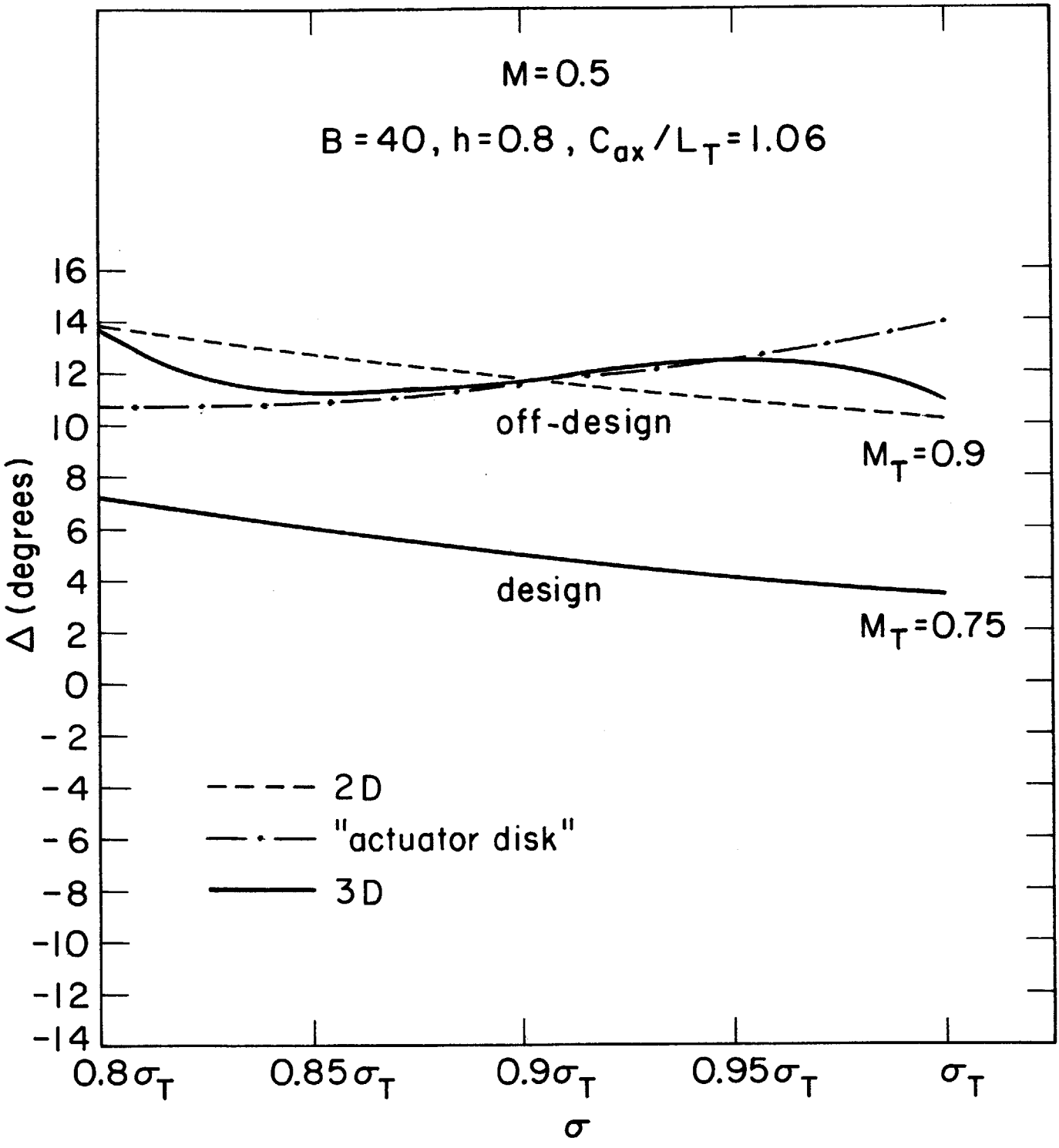
M=0.5
B=40, h=0.8, C_{ax}/L_T=1.06
16
14
12
10
8
6
4
2
0
-2
-4
-6
-8
-10
-12
-14
Δ (degrees)
off-design
M_T=0.9
design
M_T=0.75
2D
"actuator disk"
3D
0.8σ_T
0.85σ_T
0.9σ_T
0.95σ_T
σ_T
σ

Figure 7

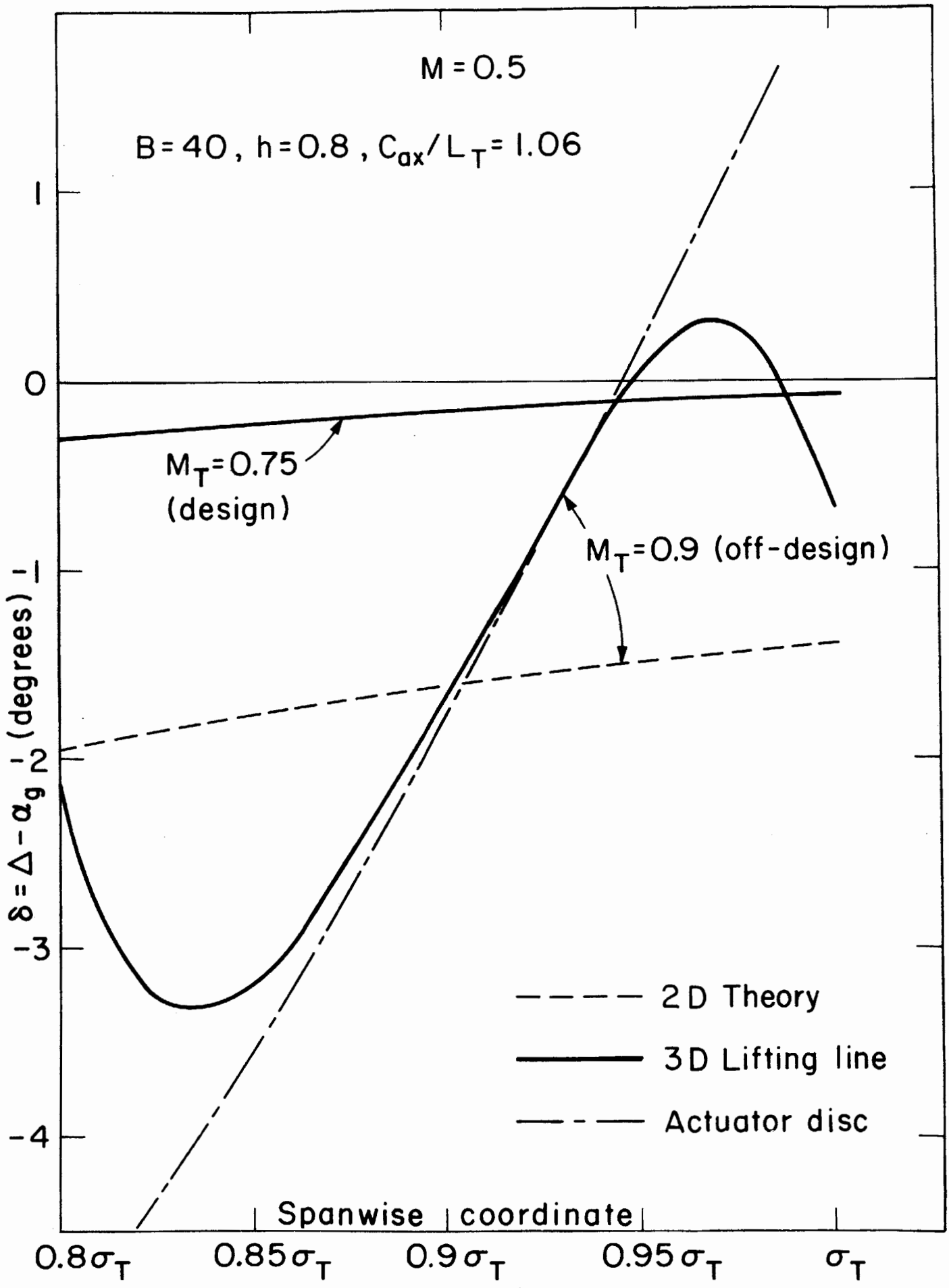
M = 0.5
B = 40 , h = 0.8 , C_{ax}/L_T = 1.06
M_T = 0.75 (design)
M_T = 0.9 (off-design)
2D Theory
3D Lifting line
Actuator disc
$-\delta = \Delta - \alpha_g$ (degrees)
Spanwise coordinate
1
0
-1
-2
-3
-4
$0.8\sigma_T$
$0.85\sigma_T$
$0.9\sigma_T$
$0.95\sigma_T$
σ_T

Figure 8

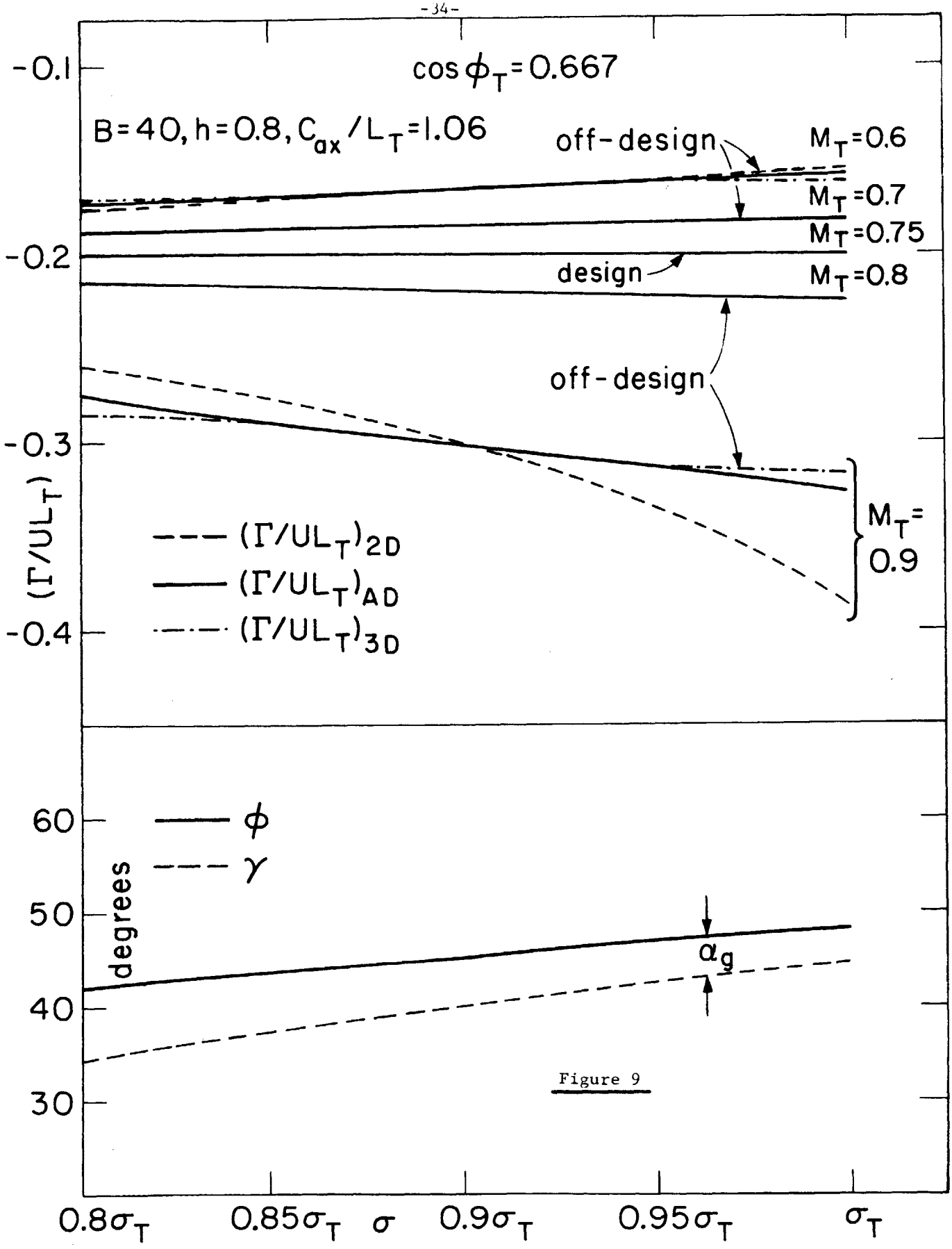
cos φT = 0.667
B = 40, h = 0.8, Cax / LT = 1.06
off-design
MT = 0.6
MT = 0.7
MT = 0.75
design
MT = 0.8
off-design
MT = 0.9
(Γ/ULT)2D
(Γ/ULT)AD
(Γ/ULT)3D
(Γ/ULT)
-0.1
-0.2
-0.3
-0.4
φ
γ
degrees
αg
60
50
40
30
0.8σT
0.85σT
σ
0.9σT
0.95σT
σT

Figure 9

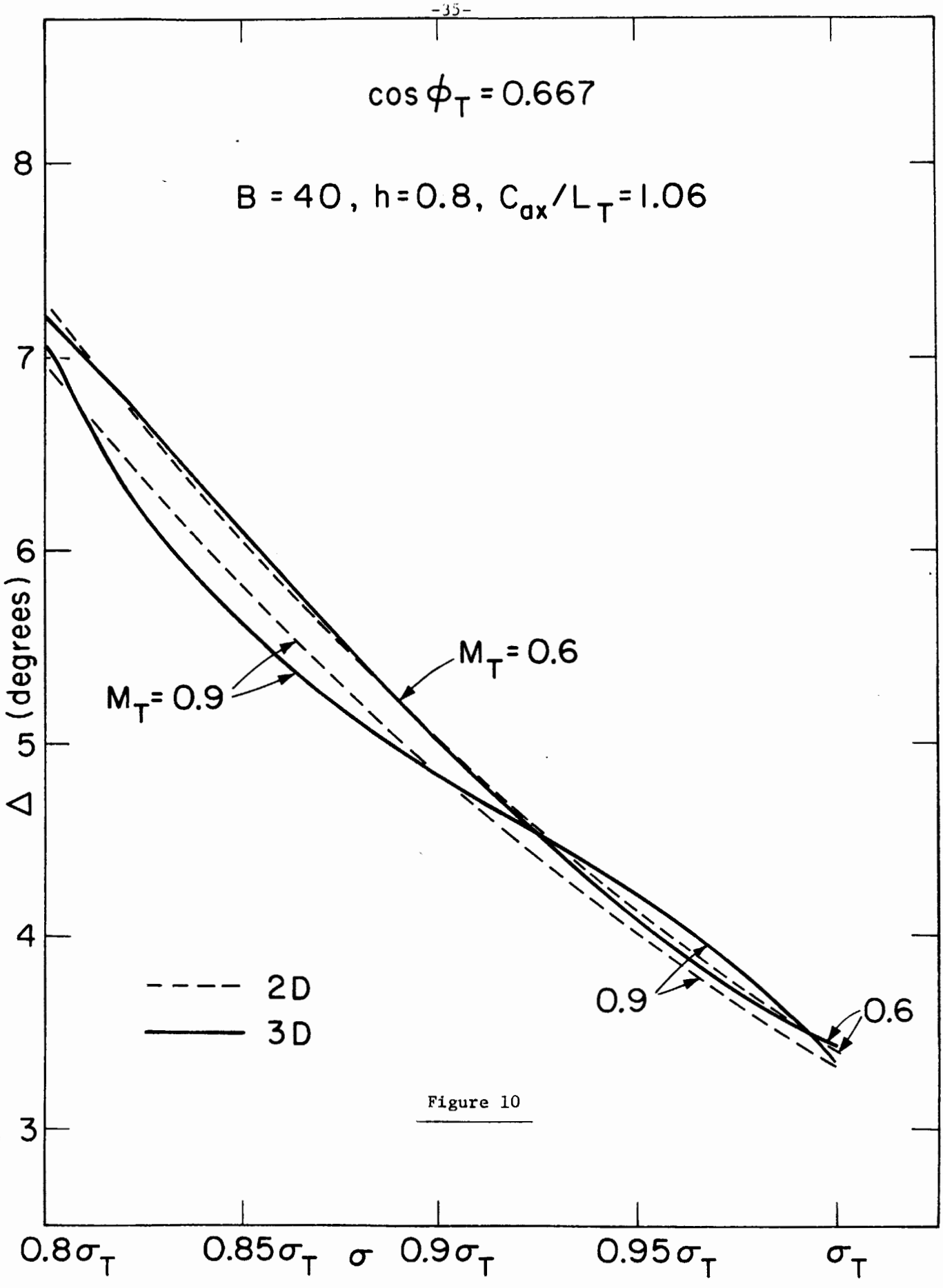
$\cos\phi_T = 0.667$
B = 40, h = 0.8, C_{ax}/L_T = 1.06
8
7
6
5
4
3
Δ σ (degrees)
M_T = 0.6
M_T = 0.9
---- 2D
—— 3D
0.9
0.6
$0.8\sigma_T$
$0.85\sigma_T$
σ
$0.9\sigma_T$
$0.95\sigma_T$
σ_T

Figure 10

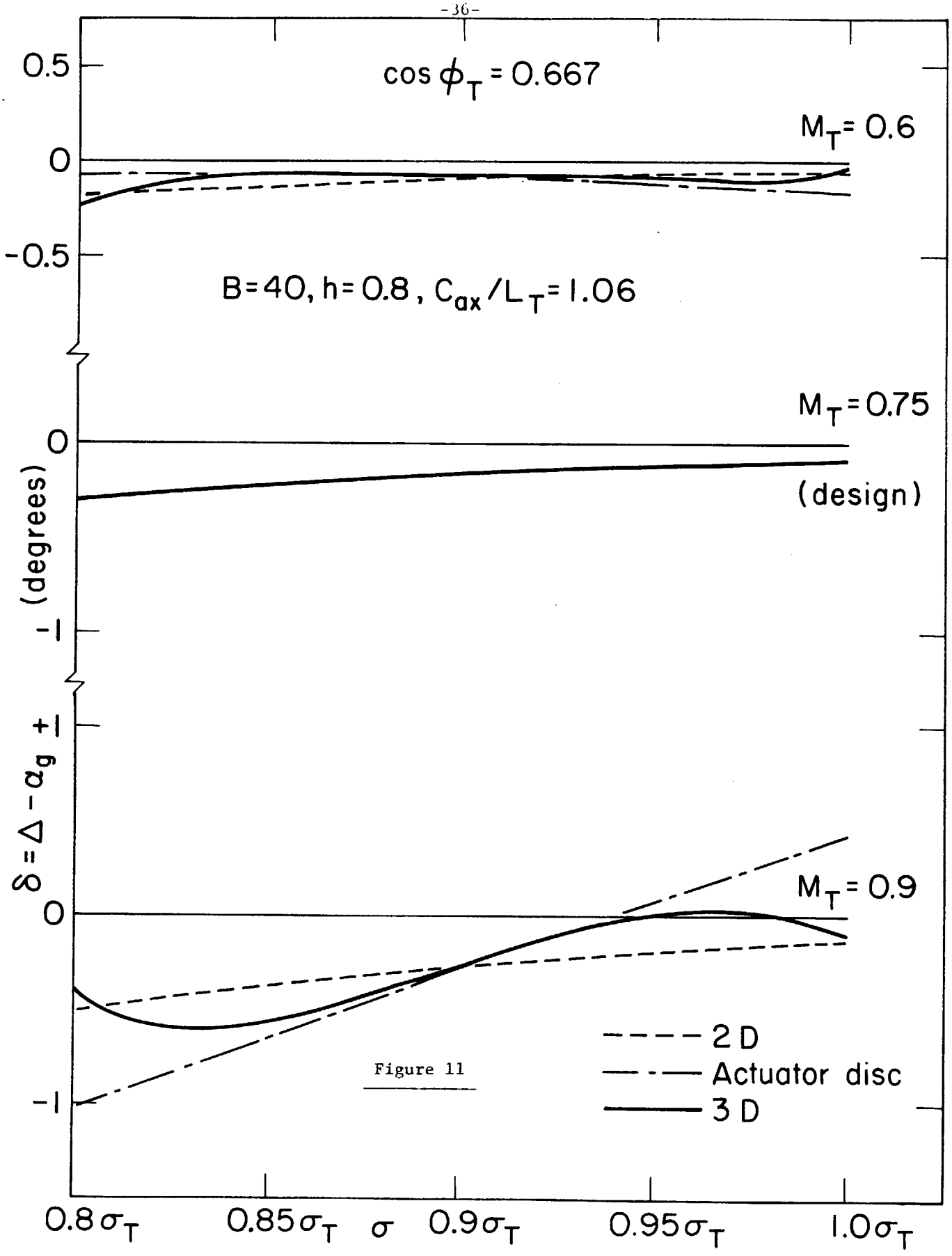
cos φT = 0.667
MT = 0.6
B=40, h=0.8, Cax/LT = 1.06
MT = 0.75
(design)
MT = 0.9
δ = Δ - αg (degrees)
2 D
Actuator disc
3 D
0.8σT
0.85σT
σ
0.9σT
0.95σT
1.0σT

Figure 11